

## Ligand-Free Nano-Grain $\text{Cu}_2\text{SnS}_3$ as a Potential Cathode Alternative for Both Cobalt and Iodine Redox Electrolyte Dye-Sensitized Solar Cells

Feng Liu<sup>a,b</sup>, Shuanglin Hu<sup>c</sup>, Xunlei Ding<sup>a</sup>, Jun Zhu<sup>\*,b</sup>, Jian Wen<sup>b</sup>, Xu Pan<sup>b</sup>, Shuanghong Chen<sup>b</sup>,  
Md. K. Nazeeruddin<sup>d</sup>, and Songyuan Dai<sup>\*,a,b</sup>

<sup>a</sup>Beijing Key Laboratory of Novel Thin Film Solar Cells, State Key Laboratory of Alternate Electrical Power System with Renewable Energy Sources, North China Electric Power University, Beijing, 102206, P. R. China

<sup>b</sup>Key Laboratory of Novel Thin Film Solar Cells, Institute of Applied Technology, Hefei Institutes of Physical Science, Chinese Academy of Sciences, Hefei, 230031, P. R. China

<sup>c</sup>Institute of Nuclear Physics and Chemistry, China Academy of Engineering Physics, Mianshan Road 64, Mianyang 621900, Sichuan, P. R. China

<sup>d</sup>Laboratory for Photonics and Interfaces, Institute of Chemical Sciences and Engineering, School of Basic Science, Swiss Federal, Institute of Technology, CH-1015 Lausanne, Switzerland

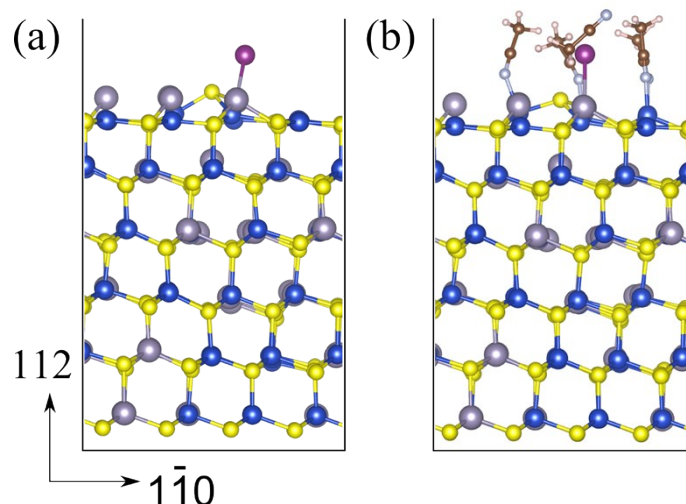


**Figure S1.** Geometry structure of the adsorption configuration of (a) one I atom with the most strong adsorption ( $E_{ad}^I = -0.95$  eV), and (b) the I adsorption configuration together with five around  $\text{CH}_3\text{CN}$  molecules ( $E_{ad}^I = -0.79$  eV) on the tetragonal  $\text{Cu}_2\text{SnS}_3$  (112) surface slab model as examples. The blue, gray, and yellow balls represent the Cu, Sn, and S atoms, respectively. The purple, cyan, brown, and white balls are I, N, C, and H, respectively.

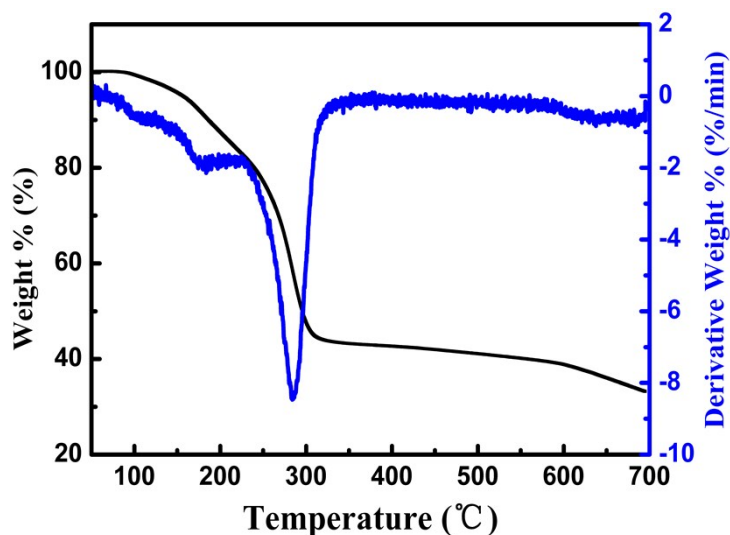


**Figure S2.** TGA trace of CTS solid precursor, obtained by pre-drying solution at 120 °C. Conditions: 60 mL min<sup>-1</sup> nitrogen, ramp 10 °C min<sup>-1</sup> to 500 °C.

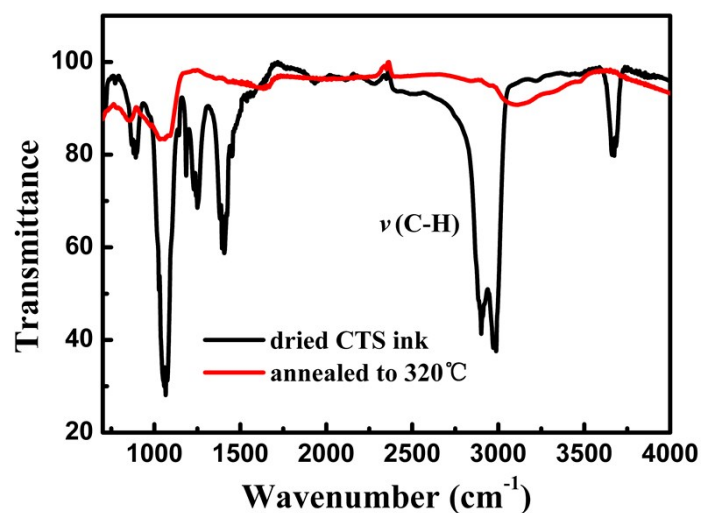


**Figure S3.** FT-IR spectra of the CTS ink dried to 120 °C for 10 min and after annealing to 320 °C. It was clear that the strong features associated with the  $\nu(\text{C-H})$  stretching bands originating from the organic species in the dried films were greatly reduced after annealing to 320 °C, indicating the significant elimination and/or decomposition of the organic species from the dried solid.

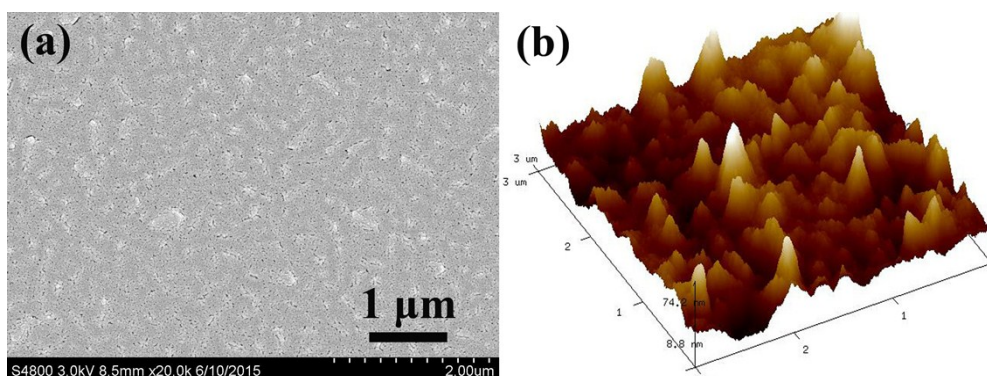


**Figure S4.** (a) Low-magnification surface SEM image and (b) AFM image of  $3\ \mu\text{m}$  by  $3\ \mu\text{m}$  surface area of the CTS thin film.

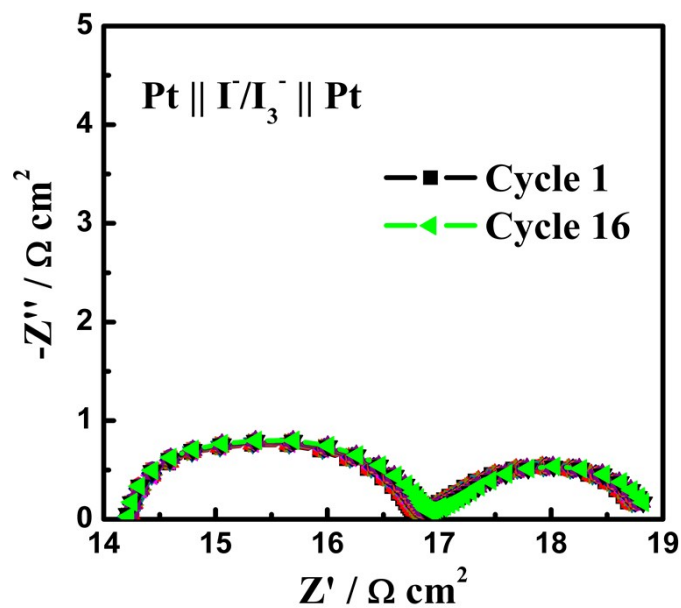


**Figure S5.** Nyquist plots of EIS for Pt symmetrical cells in iodine electrolyte. This sequential electrochemical test was repeated 16 times.

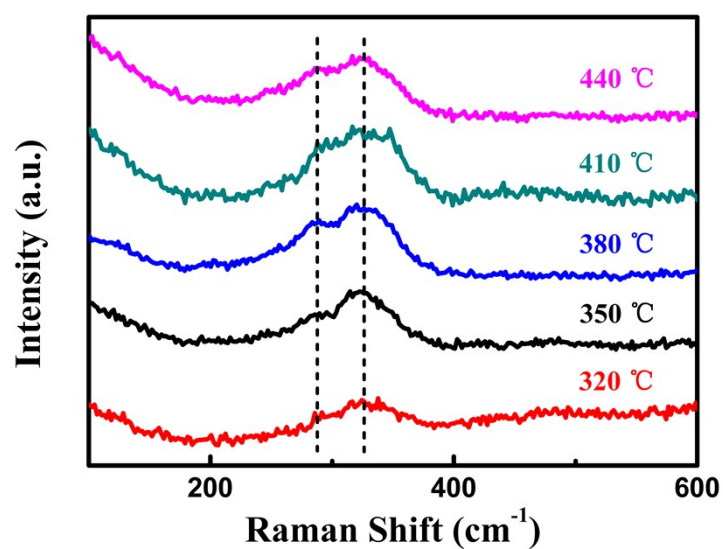


**Figure S6.** Raman spectra for the sample annealed at different final temperatures of 320 °C, 350 °C, 380 °C, 410 °C, and 440 °C.

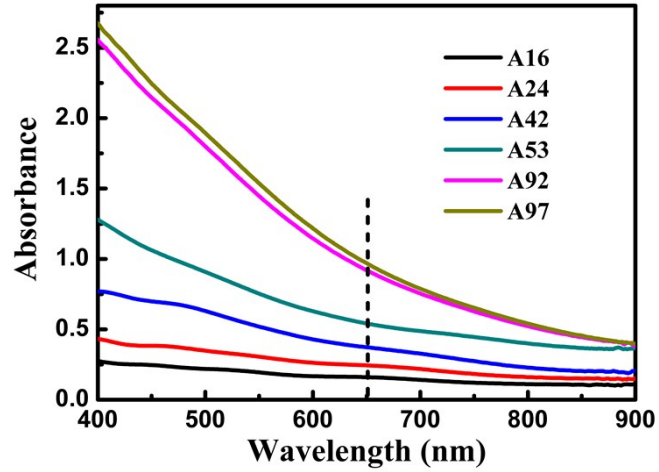


**Figure S7.** Optical absorbance of CTS films. A16, A24, A42, and A53 electrodes were prepared by spin-coating (3000 rpm, 30s) 0.05, 0.07, 0.1, 0.2 M precursor solution on a FTO glass, respectively, with a heat-treatment at 380 °C. A97 was obtained by drop-casting 0.1 M precursor solution with the same heat-treatment at 380 °C. A92 was obtained by twice spin coating/sintering 0.2 M solution on a FTO glass with the same heat-treatment at 380 °C.

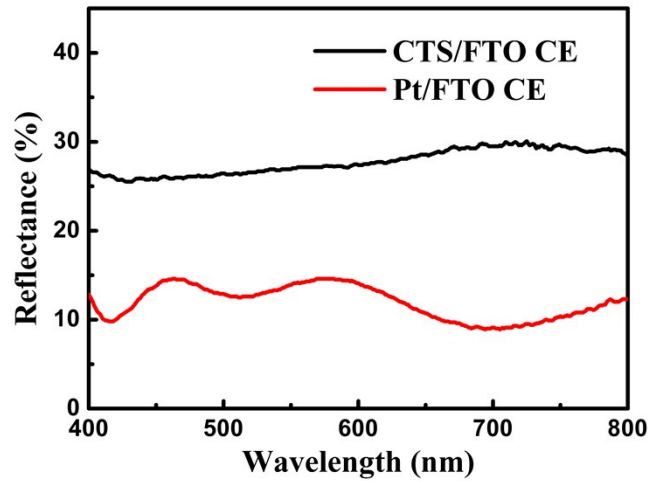


**Figure S8.** Reflectance of CTS and Pt thin film on FTO glass.

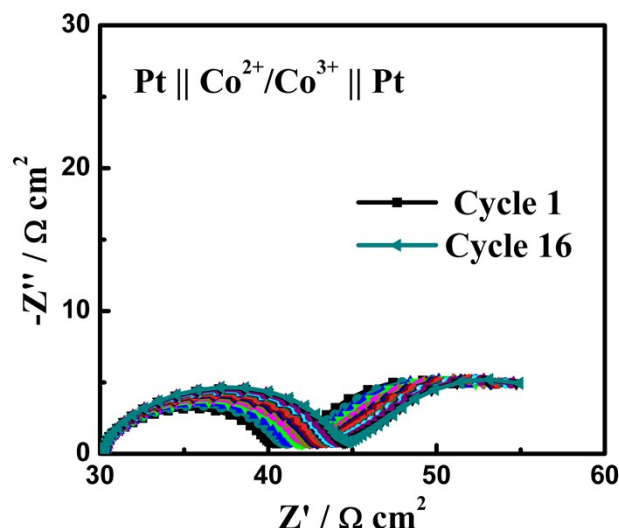


**Figure S9.** Nyquist plots of EIS for Pt symmetrical cells in cobalt electrolyte. This sequential electrochemical test was repeated 16 times.

**Table S1.** The adsorption energy and site (on Cu or Sn) of one iodine atom of all the adsorbed configurations.

| Config.        | 1  | 2  | 3  | 4  | 5  | 6  | 7  | 8  | 9  | 10 | 11 | 12 | 13 | 14 | 15 | 16 |
|----------------|----|----|----|----|----|----|----|----|----|----|----|----|----|----|----|----|
| $E_{ad}^I$ /eV | -  | -  | -  | -  | -  | -  | -  | -  | -  | -  | -  | -  | -  | -  | -  | -  |
|                | 0. | 0. | 0. | 0. | 0. | 0. | 0. | 0. | 0. | 0. | 0. | 0. | 0. | 0. | 0. | 0. |
|                | 95 | 87 | 85 | 83 | 82 | 75 | 72 | 72 | 71 | 67 | 66 | 64 | 61 | 60 | 60 | 50 |
| site           | Sn | Sn | Cu | Cu | Sn | Cu | Cu | Cu | Cu | Sn | Cu | Sn | Cu | Cu | Cu | Cu |

**Table S2.** The adsorption energy and site (on Cu or Sn) of one CH<sub>3</sub>CN molecule on the tested adsorbed configurations. The adsorption energies are calculated according to:

$$E_{ad}^{CH_3CN} = E_{tot}(CH_3CN_{(N)}/surface) - E_{tot}(CH_3CN_{(N-1)}/surface) - \frac{1}{2}E_{tot}(CH_3CN, gas).$$

Here,  $E_{tot}(CH_3CN_{(N)}/surface)$ ,  $E_{tot}(CH_3CN_{(N-1)}/surface)$ , and  $E_{tot}(CH_3CN, gas)$  are the energies of N CH<sub>3</sub>CN molecule(s) adsorbed on the Cu<sub>2</sub>SnS<sub>3</sub> surface system, the surface with the N-1 number of adsorbed CH<sub>3</sub>CN molecules, and CH<sub>3</sub>CN in the gas phase, respectively. In this table, N=1, without iodine together.

| Config.        | 1  | 2  | 3  | 4  | 5  | 6  | 7  | 8  | 9  | 10 | 11 | 12 | 13 | 14 | 15 | 16 |
|----------------|----|----|----|----|----|----|----|----|----|----|----|----|----|----|----|----|
| $E_{ad}^I$ /eV | -  | -  | -  | -  | -  | -  | -  | -  | -  | -  | -  | -  | -  | -  | -  | -  |
|                | 0. | 0. | 0. | 0. | 0. | 0. | 0. | 0. | 0. | 0. | 0. | 0. | 0. | 0. | 0. | 0. |
|                | 50 | 48 | 48 | 44 | 42 | 42 | 41 | 41 | 39 | 38 | 31 | 18 | 17 | 16 | 14 | 12 |
| site           | Cu | Cu | Cu | Cu | Cu | Sn | Cu | Cu | Cu | Cu | Cu | Sn | Sn | Sn | Sn | Sn |

**Table S3.** The adsorption energy and number (N) of CH<sub>3</sub>CN molecules referring to the lowest energy I adsorption configuration with (N-1) CH<sub>3</sub>CN molecules. There are five Cu sites around iodine atom in this I adsorption configuration. The corresponding

$E_{ad}^I$  energies are also presented.

| N | $E_{ad}^{CH_3CN}$ | $E_{ad}^I$ |
|---|-------------------|------------|
| 1 | -0.78             | -1.25      |
| 2 | -0.66             | -1.25      |
| 3 | -0.45             | -1.14      |
| 4 | -0.46             | -1.09      |
| 5 | -0.39             | -0.79      |